Specific absorption rate of assembly of magnetic nanoparticles with uniaxial anisotropy

N A Usov[1,2], E M Gubanova[2], Z H Wei[1]
[1]School of Mechanics and Engineering Science of Zhengzhou University, China
[2]National Research Nuclear University "MEPhI", 115409, Moscow, Russia
E-mail: usov@obninsk.ru (N.A. Usov, corresponding author)

Abstract. Specific absorption rate of superparamagnetic nanoparticles with uniaxial magnetic anisotropy has been calculated both for dilute assembly and for assembly of nanoparticle clusters with various filling factors using numerical simulation. The optimal particle diameters at which the specific absorption rate of assembly reaches a maximum have been obtained depending on the value of the uniaxial anisotropy constant. The optimal particle diameters are found to shift to smaller values with an increase in the anisotropy constant. The range of optimal diameters decreases simultaneously. The specific absorption rate decreases also as a function of cluster filling factor, but the optimal particle diameters remain almost unchanged.

1. Introduction

Magnetic nanoparticles have unique ability to effectively absorb the energy of a low-frequency alternating magnetic field and their surface is easily amenable to bio-functional modification. In addition, due to sufficiently small sizes magnetic nanoparticles can cross biological barriers to penetrate deep into the body tissues [1-4]. These unique properties of magnetic nanoparticles are important for biomedical applications, such as magnetic hyperthermia, enhanced contrast in magnetic resonance imaging, targeted drug delivery, purification of biological media from toxins, etc. The uses of magnetic nanoparticles for stem cell manipulation in the treatment of vascular atherosclerosis, for mechanical action on cell membranes, for food quality control, etc. are also under consideration [1-9].

Magnetic hyperthermia [3, 10-14] is one of the most promising areas in modern biomedical research related to the cancer treatment. Tumor cells are known [3, 15] to be more susceptible to the influence of elevated temperature than normal tissues. Maintaining the temperature of the affected organ above 42° C for 20-30 minutes leads to necrosis of cancer cells. It is worth mentioning that magnetic hyperthermia has a number of fundamental advantages in the cancer treatment: 1) the penetration depth of a low-frequency alternating magnetic field is much greater than that of electromagnetic radiation, 2) nanoparticles can penetrate deep into biological tissues, 3) the surface of the nanoparticles can be modified to achieve biocompatibility and to minimize the adsorption of blood proteins, 4) assemblies of superparamagnetic nanoparticles are capable of providing extremely large values of the specific absorption rate (SAR) in alternating magnetic field, of the order of 1 kW per gram of substance [16-18].

It is well known that magnetic nanoparticles of iron oxides (magnetite, maghemite) are biocompatible and have sufficiently short periods of elimination from the body [4, 14]. These significant properties, along with a sufficiently high saturation magnetization [19], make iron oxide nanoparticles excellent candidates for use in magnetic hyperthermia [4, 14, 20]. Meanwhile, an assembly of magnetic nanoparticles is a very complex physical object. Its properties are determined by a number of factors, such as the chemical composition and particle crystal structure, possible particle surface contamination,

the distribution of the particles in size and shape, etc. In addition, the character of the magnetic anisotropy of individual nanoparticles, the effect of the strong magnetic dipole interaction between the particles, and the thermal fluctuations of the magnetic moments of the particles have a great influence on the assembly properties [11-14, 21].

The only nanoparticles with a sufficiently large SAR in alternating magnetic field of moderate amplitude are suitable to be used in magnetic hyperthermia. This ensures the safety of the treatment procedure and reduces its cost. However, the SAR of nanoparticle assembly depends [11-14, 21] on the particle saturation magnetization, as well as on the value of effective anisotropy constant, the average particle diameter, etc. The proper choice of the frequency and amplitude of an alternating magnetic field is also very important. Unfortunately, in a number of experimental works [22–27] the average particle diameters and their magnetic properties turned out to be far from optimal. This leads to very small SAR, of the order of 1–10 W/g, which renders such assemblies inapplicable for use in magnetic hyperthermia.

Recent theoretical [10, 11, 21, 28-33] and experimental [16-18, 34-35] studies show that with a proper choice of the magnetic and geometric parameters of nanoparticles, one can obtain SAR values up to 1 kW/g. In this work the influence of the effective magnetic anisotropy constant on the SAR of an assembly of iron oxide nanoparticles with typical saturation magnetization M_s = 350 emu/cm^3 has been studied in detail. First, for dilute assemblies of nanoparticles the interval of optimal particle diameters, where SAR of the assembly has a large enough value, is determined as a function of the effective anisotropy constant. Then, for particles of optimal diameters the influence of the magneto -dipole interaction on the SAR in dense clusters of nanoparticles is studied depending on cluster filling factor. The SAR is found to decrease with the increase of the cluster filling factor. However, the optimal particle diameters remain almost unchanged. The results obtained are of interest for creating magnetic nanoparticle assemblies promising for use in magnetic hyperthermia.

2. Numerical simulation

2.1 Non interacting nanoparticles

For a sufficiently dilute assembly of nanoparticles with uniaxial anisotropy the calculation of low frequency hysteresis loops can be carried out using approximate kinetic equation [10] for the population numbers $n_1(t)$ and $n_2(t)$ of two potential wells of superparamagnetic nanoparticle

$$\frac{\partial n_1}{\partial t} = \frac{n_2}{\tau_2(T)} - \frac{n_1}{\tau_1(T)}; \qquad n_1(t) + n_2(t) = 1. \tag{1}$$

Here $\tau_1(T)$ and $\tau_2(T)$ are the corresponding relaxation times at a given temperature T for first and second potential wells, respectively. The equations for the relaxation times $\tau_1(T)$ and $\tau_2(T)$ that depend essentially on the amplitude and direction of the applied magnetic field with respect to particle easy anisotropy axis can be found in the appendix of reference 10. The iteration procedure can be used to calculate the well population numbers $n_1(t)$ and $n_2(t)$ and to obtain stationary hysteresis loop of a particle in alternating magnetic field. To get hysteresis loop for a dilute assembly of randomly oriented nanoparticles it is necessary to average the reduced particle magnetization over the applied magnetic field directions.

2.2. Nanoparticle clusters

To investigate the effect of the mutual magneto-dipole interaction on the SAR of assembly of interacting magnetic nanoparticles in this paper we study the behaviour of dilute assemblies of 3D clusters of superparamagnetic nanoparticles which arise usually in biological media loaded with fine magnetic nanoparticles [36, 37]. In a quasi-spherical 3D cluster of radius R_{cl} there are N_p nanoparticles of the same

diameter D. The nanoparticle centres, $\{\boldsymbol{r}_i\}$, i = 1,2, N_p, are randomly distributed in the cluster volume. Such 3D cluster is characterized by its filling factor $\eta = N_pV/V_{cl}$. Here V is the volume of nanoparticle and V_{cl} is the volume of cluster, respectively. For an assembly of random 3D clusters the orientations of the easy anisotropy axes of nanoparticles, $\{\boldsymbol{e}_i\}$, i = 1,2, N_p, are chosen randomly and independently on the unit sphere.

For a given set of initial parameters, i.e. D, R_{cl} and N_p, various random 3D clusters differ by the sets of the coordinates of the nanoparticle centres $\{\boldsymbol{r}_i\}$, and orientations $\{\boldsymbol{e}_i\}$ of the particle easy anisotropy axes. However, the calculations show that in the limit N_p>> 1 the hysteresis loops obtained for different realizations of random variables $\{\boldsymbol{r}_i\}$ and $\{\boldsymbol{e}_i\}$ differ only slightly from each other. Moreover, if one calculates a hysteresis loop averaged over a sufficiently large number of random cluster realizations, one obtains a non-random hysteresis loop. The latter characterizes the behaviour of a dilute assembly of random nanoparticle clusters.

2.3. Stochastic Landau- Lifshitz equation

Dynamics of the unit magnetization vector $\vec{\alpha}_i$ of i-th single-domain nanoparticle of the cluster is determined by the stochastic Landau – Lifshitz equation [37-41]

$$\frac{\partial \vec{\alpha}_i}{\partial t} = -\gamma_1 \vec{\alpha}_i \times \left(\vec{H}_{ef,i} + \vec{H}_{th,i}\right) - \kappa\gamma_1 \vec{\alpha}_i \times \left(\vec{\alpha}_i \times \left(\vec{H}_{ef,i} + \vec{H}_{th,i}\right)\right), \qquad i = 1,2, ..,N_p, \tag{2}$$

where γ is the gyromagnetic ratio, κ is phenomenological damping parameter, $\gamma_1 = \gamma/(1+\kappa^2)$, $\vec{H}_{ef,i}$ is the effective magnetic field and $\vec{H}_{th,i}$ is the thermal field. The effective magnetic field acting on a separate nanoparticle can be calculated as a derivative of the total cluster energy

$$\vec{H}_{ef,i} = -\frac{\partial W}{M_s V \partial \vec{\alpha}_i}. \tag{3}$$

The total magnetic energy of the cluster $W = W_a + W_Z + W_m$ is a sum of the magnetic anisotropy energy W_a, Zeeman energy W_Z of the particles in applied magnetic field, and the energy of mutual magneto-dipole interaction of the particles W_m.

For nanoparticles with uniaxial anisotropy the magnetic anisotropy energy is given by

$$W_a = KV\left(1 - \left(\vec{\alpha}\vec{e}\right)^2\right), \tag{4}$$

where K is the effective anisotropy constant and $\boldsymbol{e}$ is the unit vector along the easy axis direction. Next, Zeeman energy of the cluster in applied alternating magnetic field is given by

$$W_Z = -M_s V \sum_{i=1}^{N_p} \left(\vec{\alpha}_i \vec{H}_0 \sin(\omega t)\right), \tag{5}$$

where $\omega = 2\pi f$ is the angular frequency.

For nearly spherical uniformly magnetized nanoparticles the magnetostatic energy of the cluster can be represented as the energy of the point interacting dipoles located at the particle centres $\boldsymbol{r}_i$ within the cluster. Then the energy of magneto-dipole interaction is

$$W_m = \frac{M_s^2 V^2}{2} \sum_{i \neq j} {}_j \frac{\vec{\alpha}_i \vec{\alpha}_j - 3\left(\vec{\alpha}_i \vec{n}_{ij}\right)\left(\vec{\alpha}_j \vec{n}_{ij}\right)}{\left|\vec{r}_i - \vec{r}_j\right|^3}, \tag{6}$$

where $\boldsymbol{n}_{ij}$ is the unit vector along the line connecting the centres of *i*-th and *j*-th particles, respectively.

The thermal fields $\vec{H}_{th,i}$ acting on various nanoparticles of the cluster are statistically independent, with the following statistical properties [38] of their components

$$\left\langle H_{th.i}^{(\alpha)}(t)\right\rangle = 0\,; \qquad \left\langle H_{th,i}^{(\alpha)}(t)H_{th,i}^{(\beta)}(t_1)\right\rangle = \frac{2k_B T\kappa}{\gamma M_s V}\delta_{\alpha\beta}\delta(t-t_1), \quad \alpha,\beta = (x,y,z). \qquad (7)$$

Here k_B is the Boltzmann constant, $\delta_{\alpha\beta}$ is the Kroneker's symbol, and $\delta(t)$ is the delta function.

3. Results and discussion

3.1. Non interacting nanoparticles

Let us first discuss the results of SAR calculation for dilute assemblies of superparamagnetic nanoparticles obtained using the approximate kinetic equation (1). It was previously shown [10] that the results obtained using this approach coincide up to several percents with the calculations based on the stochastic Landau – Lifshitz equation (2), neglecting the magnetic dipole interaction of nanoparticles. Due to high performance of the approximate kinetic equation (1), one can study in detail the effect of changes in the magnetic parameters and average sizes of nanoparticles on the SAR of assembly. However, this approach does not take into account the influence of the magnetic dipole interaction on the dynamics of particle magnetic moments. Therefore, the results described in this paragraph are applicable only for the analysis of experimental data obtained for sufficiently dilute assemblies of magnetic nanoparticles.

The saturation magnetization for iron oxide nanoparticles is known to be in the range M_s = 300 – 400 emu/cm^3 [18, 42-49], depending on the oxide chemical composition and its uniformity. For simplicity, in this work the saturation magnetization of iron oxide nanoparticles is taken to be M_s = 350 emu/cm^3. At the same time, due to distortion of the spherical shape and inhomogeneous crystal structure the effective magnetic anisotropy constant of nanoparticles can vary in a much wider range, from 8×10^4 to 5×10^5 erg/cm^3 [18, 42-49]. In addition, in the experimentally studied assemblies there is a significant scatter in particle diameters. Therefore, in this work we considered assemblies of particles with various effective anisotropy constants in a wide range of average diameters, from 10 to 50 nm. The latter, however, do not exceed the single domain diameter of an iron oxide nanoparticle. Due to the large set of parameters that determine the SAR value, the alternating magnetic field frequency is fixed at a typical value f = 300 kHz, while the amplitude of the alternating magnetic field varied in the range H_0 = 100 – 200 Oe.

Figure 1 shows the examples of low-frequency hysteresis loops of dilute randomly oriented assemblies of magnetic nanoparticles obtained using approximate kinetic equation (1).

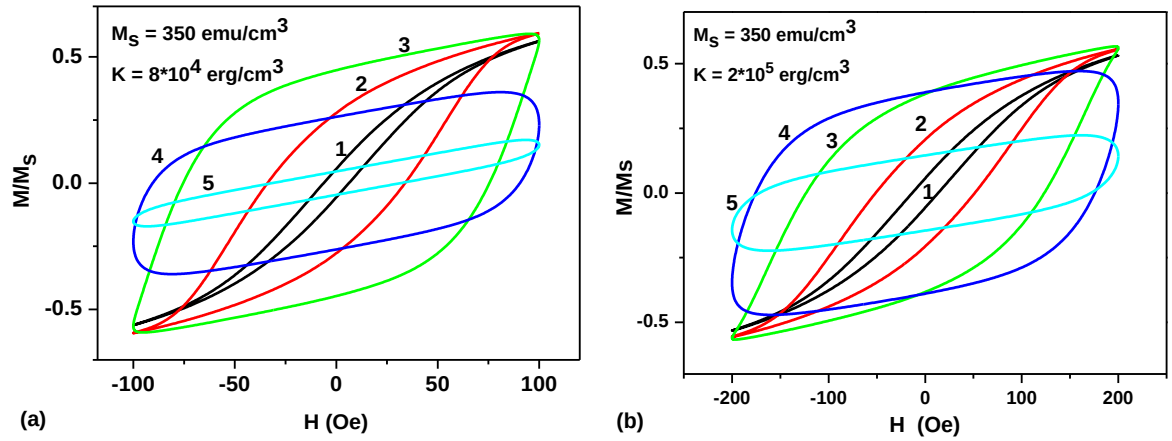

Figure 1. a) Low frequency hysteresis loopsof random assembly of uniaxial nanoparticles for the case H_0 = 100 Oe, f = 300 kHz, K= 8×10^4 erg/cm^3 for various average diameters: 1) D = 18 nm, 2) D = 20 nm, 3) D = 22 nm, 4) D = 24 nm, 5) D = 26 nm. b) The same for the case H = 200 Oe, f = 300 kHz, K = 2×10^5 erg/cm^3; the average diameters are: 1) D = 14 nm, 2) D = 15 nm, 3) D = 16 nm, 4) D = 17 nm, 5) D = 18 nm.

It is easy to see that the hysteresis loop area substantially depends on the average particle diameter for all cases investigated. The maximal area of hysteresis loops shown in figure 1a corresponds to particles with diameter D_{max}= 22 nm, whereas for hysteresis loops shown in figure 1b the maximal area corresponds to particles with D_{max} = 16.5 nm. It is well-known [50], that the thermal power released per unit particle volume is determined by the integral

$$P = M_s f \oint \vec{\alpha} d\vec{H} = fA, \qquad (8)$$

where$A$ is the hysteresis loop area in the variables (M, H). SAR per unit mass is then given by P/ρ, where ρ is the particle density. For iron oxide nanoparticles the density ρ = 5.0 g/cm^3 is usually accepted. Knowing the area of the assembly hysteresis loop and using equation (8) one can calculate the dependence of SAR on the average particle diameter for assemblies with different values of the effective anisotropy constant. These calculations are presented in figure 2. As figure 2 shows, for each value of the effective magnetic anisotropy constant there is a rather narrow interval of optimum particle diameters where SAR of the assembly reaches maximum values.

It is easy to see that with an increase in the effective anisotropy constant, the domain of optimal particle diameters shifts toward smaller particle sizes. Simultaneously, the maximum SAR of the assembly and the range of optimal particle diameters considerably decrease. For the assemblies studied the maximum SAR values are achieved for effective anisotropy constants K = 10^{5}erg/cm^3, and K = 8×10^{4}erg/cm^3, respectively. For the case of K = 10^{5}erg/cm^3 (curve 5 in figure 2) the range of optimal particle diameters is given by 20 – 30 nm, the maximal SAR being 650 W/g. On the other hand, for particles with K = 8×10^4 erg/cm^3 (curve 6 in figure 2) the optimal particle diameters correspond to the interval 20 – 45 nm with maximal SAR equals 630 W/g.

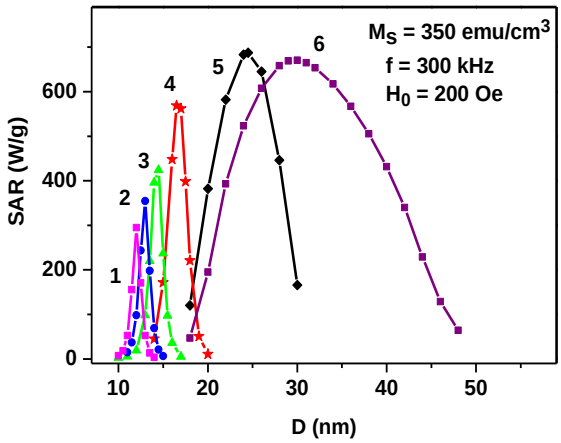

Figure 2. The dependence of SAR on the average particle diameter for various effective anisotropy constants: 1) $K = 5\times10^5$erg/cm^3, 2) $K = 4\times10^5$erg/cm^3, 3) $K = 3\times10^5$erg/cm^3, 4) $K = 2\times10^5$erg/cm^3, 5) $K = 10^5$erg/cm^3, 6) $K = 8\times10^4$erg/cm^3.

Therefore, one can see that for assemblies of particles that correspond to curves 5 and 6 in figure 2, the domains of optimal diameters are rather wide and maximal SAR reaches sufficiently high values even for moderate amplitude of alternating magnetic field. This indicates the preference of soft magnetic nanoparticles for use in magnetic hyperthermia. Similar SAR calculations can also be performed for dilute assemblies of nanoparticles with other saturation magnetization values in a wide range of alternating magnetic field frequencies and amplitudes.

3.2. Assembly of nanoparticle clusters

The results of SAR calculations given in the previous paragraph correspond to dilute assemblies of magnetic nanoparticles, which is rare situation in practice. The properties of dense assemblies of magnetic nanoparticles that usually spontaneously form in biological media [36,37] are significantly affected by the strong magneto-dipole interaction between the particles of the assembly [29-35]. The influence of the magneto- dipole interaction on the SAR of a dilute assembly of 3D nanoparticle clusters has been studied in this work by solving the stochastic Landau – Lifshitz equation (2). As an example, figure 3 demonstrates the change in the SAR with increase in the cluster filling factor η.

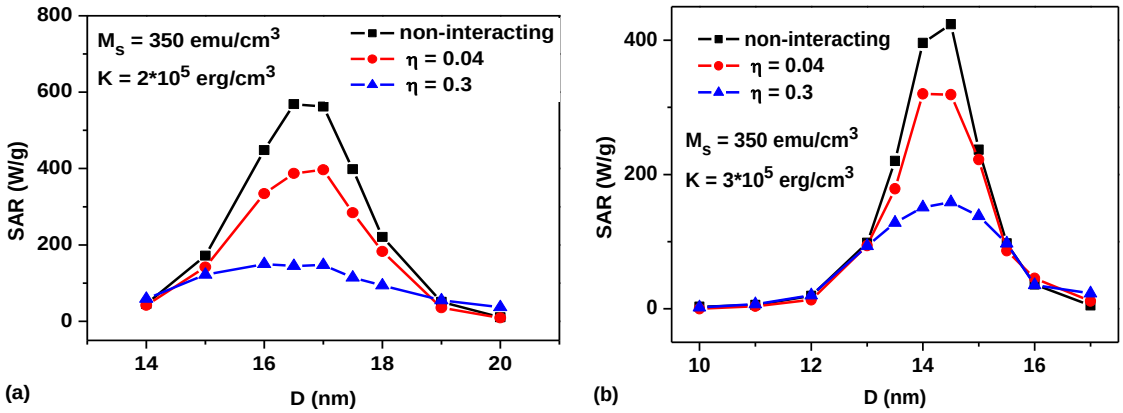

Figure 3. The dependence of SAR on particle diameter for different cluster filling factors and various particle anisotropy constants: a) $K = 2\times10^5$ erg/cm^3; b) $K = 3\times10^5$ erg/cm^3.

Evidently, with an increase in this parameter, the average distance between the nanoparticles decreases, and accordingly, the intensity of the magnetic dipole interaction in the cluster increases. As

figure 3 shows, for both cases studied, $K = 2\times10^5$ erg/cm^3 (figure 3a), and $K = 3\times10^5$ erg/cm^3 (figure 3b), the SAR of the assembly rapidly decreases as a function of cluster filling factor η. It is interesting to note, however, that the interval of optimal particle diameters, where the assembly SAR reaches high enough values, remains practically unchanged.

4. Conclusions

In this paper the low-frequency hysteresis loops and SAR in alternating magnetic field have been calculated for assemblies of magnetic nanoparticles with uniaxial anisotropy. For dilute assemblies of nanoparticles where influence of magneto-dipole interaction is negligibly small the optimal range of particles, where SAR of the assembly has sufficiently large value, has been determined depending on the value of effective anisotropy constant. It is found that the range of optimal particle diameters decreases as a function of effective anisotropy constant. The maximal SAR values, of the order of 600 – 650 W/g, have been obtained for soft magnetic particles with effective anisotropy constants in the range $K = 8\times10^4$ - 10^5 erg/cm^3. However SAR decreases nearly twice when effective anisotropy constant increases from $K = 8\times10^4$ erg/cm^3 up to $K = 5\times10^5$erg/cm^3.

The SAR of a dilute assembly of dense nanoparticle clusters decreases considerably with increasing the cluster filling factor η. However, the interval of optimal particle diameters does not depend considerably on the value of this parameter.

References

[1] Fratila R, Martínez J F 2019 *Nanomaterials for Magnetic and Optical Hyperthermia Applications* (Elsevier).
[2] Cardoso V F, Francesko A, Ribeiro C, Bañobre-López M, Martins P and Lanceros-Mendez S Advances in Magnetic Nanoparticles for Biomedical Applications 2017 *Advanced Healthcare Materials* **7** 1700845.
[3] Pankhurst Q A, Thanh N T K, Jones S K and Dobson J Progress in applications of magnetic nanoparticles in biomedicine 2009 *Journal of Physics D: Applied Physics* **42** 224001.
[4] Silva A et. al. 2016 *Medical applications of iron oxide nanoparticles Iron Oxides: From Nature to Applications* ed D Faivre (Wiley-VCH Verlag) pp. 425 – 471.
[5] Mou X, Ali Z, Li S and He N Applications of Magnetic Nanoparticles in Targeted Drug Delivery System 2015 *Journal of Nanoscience and Nanotechnology* **15** 54–62.
[6] Vaghari H, Jafarizadeh-Malmiri H, Mohammadlou M, Berenjian A, Anarjan N, Jafari N and Nasiri S Application of magnetic nanoparticles in smart enzyme immobilization 2015 *Biotechnology Letters* **38** 223–33.
[7] Mohammed L, Gomaa H G, Ragab D and Zhu J Magnetic nanoparticles for environmental and biomedical applications: A review 2017 *Particuology* **30** 1–14.
[8] Reddy L H, Arias J L, Nicolas J and Couvreur P Magnetic Nanoparticles: Design and Characterization, Toxicity and Biocompatibility, Pharmaceutical and Biomedical Applications 2012 *Chemical Reviews* **112** 5818–78.
[9] Wierucka M and Biziuk M Application of magnetic nanoparticles for magnetic solid-phase extraction in preparing biological, environmental and food samples TrAC 2014 *Trends in Analytical Chemistry* **59** 50–8.
[10] Usov N A Low frequency hysteresis loops of superparamagnetic nanoparticles with uniaxial anisotropy 2010 *Journal of Applied Physics* **107** 123909.
[11] Carrey J, Mehdaoui B and Respaud M Simple models for dynamic hysteresis loop calculations of magnetic single-domain nanoparticles: Application to magnetic hyperthermia optimization 2011 *Journal of Applied Physics* **109** 83921.
[12] Ortega D and Pankhurst Q A Magnetic hyperthermia 2013 *Nanoscience* (Royal Society of Chemistry) pp 60–88.

[13] Dutz S and Hergt R Magnetic nanoparticle heating and heat transfer on a microscale: Basic principles, realities and physical limitations of hyperthermia for tumour therapy 2013 *International Journal of Hyperthermia* **29** 790–800.
[14] Périgo E A, Hemery G, Sandre O, Ortega D, Garaio E, Plazaola F and Teran F J Fundamentals and advances in magnetic hyperthermia 2015 *Applied Physics Reviews* **2** 41302.
[15] Yu J, Huang D-Y, Yousaf M Z, Hou Y-L and Gao S Magnetic nanoparticle-based cancer therapy 2013 *Chinese Physics B* **22** 27506.
[16] Hergt R, Hiergeist R, Zeisberger M, Schüler D, Heyen U, Hilger I and Kaiser W A Magnetic properties of bacterial magnetosomes as potential diagnostic and therapeutic tools 2005 *Journal of Magnetism and Magnetic Materials* **293** 80–6.
[17] Mehdaoui B, Meffre A, Carrey J, Lachaize S, Lacroix L-M, Gougeon M, Chaudret B and Respaud M Optimal Size of Nanoparticles for Magnetic Hyperthermia: A Combined Theoretical and Experimental Study 2011 *Advanced Functional Materials* **21** 4573–81.
[18] Bonvin D, Alexander D, Millán A, Piñol R, Sanz B, Goya G, Martínez A, Bastiaansen J, Stuber M, Schenk K, Hofmann H and MionićEbersold M Tuning Properties of Iron Oxide Nanoparticles in Aqueous Synthesis without Ligands to Improve MRI Relaxivity and SAR 2017 *Nanomaterials* **7** 225.
[19] Chikazumi S 1964 *Physics of magnetism* (New York: Wiley).
[20] Kolosnjaj-Tabi J, Lartigue L, Javed Y, Luciani N, Pellegrino T, Wilhelm C, Alloyeau D and Gazeau F Biotransformations of magnetic nanoparticles in the body 2016 *Nano Today* **11** 280–4.
[21] Usov N A Iron Oxide Nanoparticles for Magnetic Hyperthermia 2019 *SPIN* **9** 1940001.
[22] Evans B A, Bausch M D, Sienerth K D and Davern M J Non-monotonicity in the influence of nanoparticle concentration on SAR in magnetic nanoparticle hyperthermia 2018 *Journal of Magnetism and Magnetic Materials* **465** 559–65.
[23] Shaterabadi Z, Nabiyouni G and Soleymani M Optimal size for heating efficiency of superparamagnetic dextran-coated magnetite nanoparticles for application in magnetic fluid hyperthermia 2018 *Physica C: Superconductivity and its Applications* **549** 84–7.
[24] Ebrahimisadr S, Aslibeiki B and Asadi R Magnetic hyperthermia properties of iron oxide nanoparticles: The effect of concentration 2018 *Physica C: Superconductivity and its Applications* **549** 119–21.
[25] Yang F, Skripka A, Tabatabaei M S, Hong S H, Ren F, Benayas A, Oh J K, Martel S, Liu X, Vetrone F and Ma D Multifunctional Self-Assembled Supernanoparticles for Deep-Tissue Bimodal Imaging and Amplified Dual-Mode Heating Treatment 2019 *ACS Nano* **13** 408–20.
[26] Linh P H, Phuc N X, Hong L V, Uyen L L, Chien N V, Nam P H, Quy N T, Nhung H T M, Phong P T and Lee I-J Dextran coated magnetite high susceptibility nanoparticles for hyperthermia applications 2018 *Journal of Magnetism and Magnetic Materials* **460** 128–36.
[27] Lemal P, Balog S, Geers C, Taladriz-Blanco P, Palumbo A, Hirt A M, Rothen-Rutishauser B and Petri-Fink A Heating behavior of magnetic iron oxide nanoparticles at clinically relevant concentration 2019 *Journal of Magnetism and Magnetic Materials* **474** 637–42.
[28] Mehdaoui B, Tan R P, Meffre A, Carrey J, Lachaize S, Chaudret B and Respaud M Increase of magnetic hyperthermia efficiency due to dipolar interactions in low-anisotropy magnetic nanoparticles: Theoretical and experimental results 2013 *Physical Review B* **87**.
[29] Landi G T Role of dipolar interaction in magnetic hyperthermia 2014 *Physical Review B* **89**.
[30] Tan R P, Carrey J and Respaud M Magnetic hyperthermia properties of nanoparticles inside lysosomes using kinetic Monte Carlo simulations: Influence of key parameters and dipolar interactions, and evidence for strong spatial variation of heating power 2014 *Physical Review B* **90**.
[31] Usov N A, Serebryakova O N and Tarasov V P Interaction Effects in Assembly of Magnetic Nanoparticles 2017 *Nanoscale Research Letters* **12**.
[32] Ruta S, Chantrell R and Hovorka O Unified model of hyperthermia via hysteresis heating in systems of interacting magnetic nanoparticles 2015 *Scientific Reports* **5**.

[33] Usov N A, Nesmeyanov M S, Gubanova E M and Epshtein N B Heating ability of magnetic nanoparticles with cubic and combined anisotropy 2019 *Beilstein Journal of Nanotechnology***10** 305–14.
[34] Sanz B, Calatayud M P, De Biasi E, Lima E, Mansilla M V, Zysler R D, Ibarra M R and Goya G F In Silico before In Vivo: how to Predict the Heating Efficiency of Magnetic Nanoparticles within the Intracellular Space 2016 *Scientific Reports* **6.**
[35] Conde-Leboran I, Baldomir D, Martinez-Boubeta C, Chubykalo-Fesenko O, del Puerto Morales M, Salas G, Cabrera D, Camarero J, Teran F J and Serantes D A Single Picture Explains Diversity of Hyperthermia Response of Magnetic Nanoparticles 2015 *The Journal of Physical Chemistry C* **119** 15698–706.
[36] Etheridge M L, Hurley K R, Zhang J, Jeon S, Ring H L, Hogan C, Haynes C L, Garwood M and Bischof J C Accounting for biological aggregation in heating and imaging of magnetic nanoparticles 2014 *TECHNOLOGY* **2** 214–28.
[37] Jeon S, Hurley K R, Bischof J C, Haynes C L and Hogan C J Quantifying intra- and extracellular aggregation of iron oxide nanoparticles and its influence on specific absorption rate 2016 *Nanoscale* **8** 16053–64.
[38] Brown W F Thermal Fluctuations of a Single-Domain Particle 1963 *Physical Review* **130** 1677–86.
[39] García-Palacios J L and Lázaro F J Langevin-dynamics study of the dynamical properties of small magnetic particles 1998 *Physical Review B* **58** 14937–58.
[40] Scholz W, Schrefl T and Fidler J Micromagnetic simulation of thermally activated switching in fine particles 2001 *Journal of Magnetism and Magnetic Materials* **233** 296–304.
[41] Coffey W T, Kalmykov Y P and Waldron J T 2004 *The Langevin Equation World Scientific Series in Contemporary Chemical Physics* vol 14, Second Edition (World Scientific) p 704.
[42] Ramirez-Nuñez A L, Jimenez-Garcia L F, Goya G F, Sanz B and Santoyo-Salazar J In vitro magnetic hyperthermia using polyphenol-coated Fe3O4@γFe2O3 nanoparticles from Cinnamomunverum and Vanilla planifolia: the concert of green synthesis and therapeutic possibilities 2018 *Nanotechnology***29** 74001.
[43] Espinosa A, Kolosnjaj-Tabi J, Abou-Hassan A, Plan Sangnier A, Curcio A, Silva A K A, Di Corato R, Neveu S, Pellegrino T, Liz-Marzán L M and Wilhelm C Magnetic (Hyper)Thermia or Photothermia? Progressive Comparison of Iron Oxide and Gold Nanoparticles Heating in Water, in Cells, and In Vivo 2018 *Advanced Functional Materials* **28** 1803660.
[44] Orozco-Henao J M, Coral D F, Muraca D, Moscoso-Londoño O, Mendoza Zélis P, Fernandez van Raap M B, Sharma S K, Pirota K R and Knobel M Effects of Nanostructure and Dipolar Interactions on Magnetohyperthermia in Iron Oxide Nanoparticles 2016 *The Journal of Physical Chemistry C* **120** 12796–809.
[45] Engelmann U M, Shasha C, Teeman E, Slabu I and Krishnan K M Predicting size-dependent heating efficiency of magnetic nanoparticles from experiment and stochastic Néel-Brown Langevin simulation 2019 *Journal of Magnetism and Magnetic Materials* **471** 450–6.
[46] Rivas Rojas P C, Tancredi P, MoscosoLondoño O, Knobel M and Socolovsky L M Tuning dipolar magnetic interactions by controlling individual silica coating of iron oxide nanoparticles 2018 *Journal of Magnetism and Magnetic Materials* **451** 688–96.
[47] Krajewski M, Brzozka K, Tokarczyk M, Kowalski G, Lewinska S, Slawska-Waniewska A, Lin W S and Lin H M Impact of thermal oxidation on chemical composition and magnetic properties of iron nanoparticles 2018 *Journal of Magnetism and Magnetic Materials* **458** 346–54.
[48] Jonasson C, Schaller V, Zeng L, Olsson E, Frandsen C, Castro A, Nilsson L, Bogart L K, Southern P, Pankhurst Q A, Puerto Morales M and Johansson C Modelling the effect of different core sizes and magnetic interactions inside magnetic nanoparticles on hyperthermia performance 2019 *Journal of Magnetism and Magnetic Materials* **477** 198–202.

[49] Roca A G, Gutiérrez L, Gavilán H, Fortes Brollo M E, Veintemillas-Verdaguer S and Morales M del P Design strategies for shape-controlled magnetic iron oxide nanoparticles 2019 *Advanced Drug Delivery Reviews* **138** 68–104.
[50] Landau L D and Lifshitz E M 1960 *Electrodynamics of Continuous Media* (London: Pergamon Press).